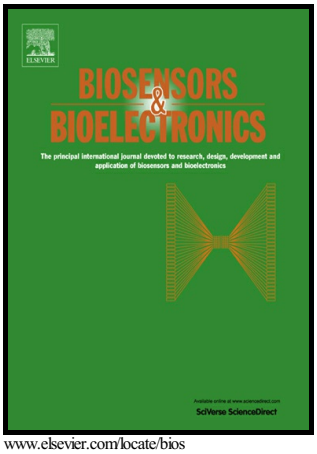

www.elsevier.com/locate/bios

Oligonucleotide-Modulated Photocurrent Enhancement of A Tetracationic Porphyrin for Label-free Homogeneous Photoelectrochemical Biosensing

Qing Hong, Lei Ge, Wenxiao Wang, Xiaojuan Liu, Feng Li

PII: S0956-5663(18)30681-X
DOI: https://doi.org/10.1016/j.bios.2018.08.071
Reference: BIOS10735

To appear in: *Biosensors and Bioelectronic*

Received date: 14 August 2018
Accepted date: 29 August 2018

Cite this article as: Qing Hong, Lei Ge, Wenxiao Wang, Xiaojuan Liu and Feng Li, Oligonucleotide-Modulated Photocurrent Enhancement of A Tetracationic Porphyrin for Label-free Homogeneous Photoelectrochemical Biosensing, *Biosensors and Bioelectronic,* https://doi.org/10.1016/j.bios.2018.08.071

Oligonucleotide-Modulated Photocurrent Enhancement of A Tetracationic Porphyrin for Label-free Homogeneous Photoelectrochemical Biosensing

Qing Hong, Lei Ge,* Wenxiao Wang, Xiaojuan Liu, and Feng Li*

College of Chemistry and Pharmaceutical Sciences, Qingdao Agricultural University, Qingdao, 266109, People's Republic of China

*Corresponding author: Lei Ge, Feng Li

E-mail: lge@qau.edu.cn, lifeng@qau.edu.cn

Telephone: +86-532-86080855

ABSTRACT

This work reports the first demonstration of an oligonucleotide-modulated label-free homogeneous photoelectrochemical (PEC) biosensing platform based on the adsorption of tetracationic porphyrin (denoted as TMPyP here) onto 1-naphthalenesulfonate anion (NS^-)-grafted indium tin oxide electrode (denoted as TMPyP-NS^--ITO), which generates a stable and rapid photocurrent response. We found that when NS^--ITO electrode was subjected to single-stranded oligonucleotide (ssON) before TMPyP adsorption, a remarkable enhancement of photocurrent intensity was observed from the resulted TMPyP-ssON-NS^--ITO electrode with high specificity towards oligonucleotide. A series of investigations were carried out to understand the mechanism of this oligonucleotide-modulated photocurrent

enhancement phenomenon. Moreover, the studies of this robust photocurrent enhancement mechanism was successfully extended to develop a signal-on homogeneous PEC biosensing platform for, as a proof-of-concept, label-free M.SssI methyltransferase activity analysis through a judiciously and compatibly engineered signal transduction strategy consisted of hairpin-shaped oligonucleotide probe, restriction endonuclease HpaII, and Exonuclease I. The rationally designed homogeneous PEC biosensor exhibit sensitive PEC response toward M.SssI methyltransferase with a low detection limit of 3.5 mU/mL and a wide linear range from 0.01 to 120 U/mL. Additionally, we show that our homogeneous PEC biosensing platform can be also utilized to screen methyltransferase inhibitors. Therefore, this work will provide a distinctive paradigm for versatile homogeneous PEC biosensing platform that can be used as potential powerful tool toward innovative label-free bioanalytical purposes.

Graphical Abstract

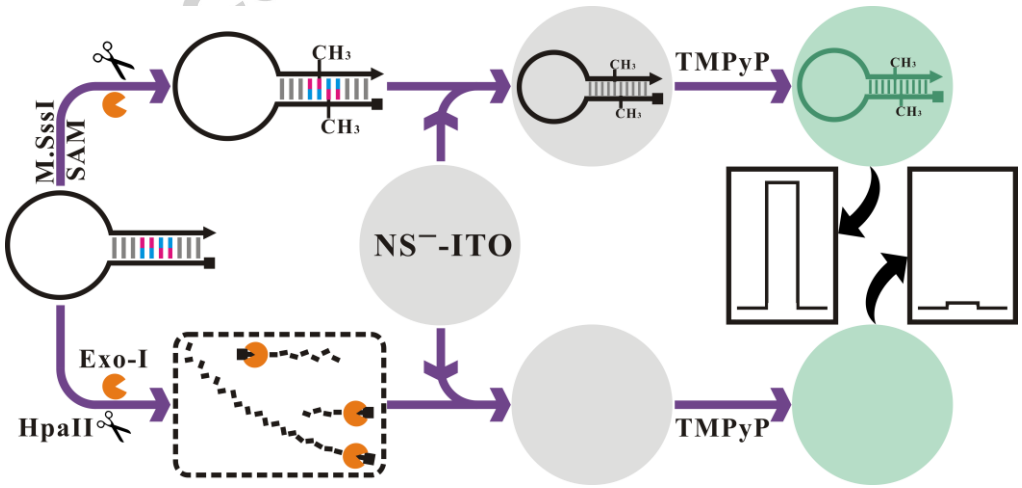

KEYWORDS: homogeneous photoelectrochemical assay; tetracationic porphyrin; label-free; methyltransferase activity analysis

1. Introduction

By integrating the electrochemical method with an optical technique, the emerged and booming photoelectrochemical (PEC) assay (Zang et al., 2017; Zhao et al., 2014b) are able to maintain the advantages of both methods and minimize their shortcomings, resulting in the significantly improved signal-to-noise ratio and sensitivity compared with the individual techniques due to the complete separation of excitation source (light) and detection signal (photocurrent) (Jiang et al., 2017; Li et al., 2017; Mei et al., 2017; Tu et al., 2016; Zheng et al., 2016). Moreover, the simple instrumentation, fast response, easy miniaturization, and low cost of the electrochemical signal readout in PEC strategies have further aroused considerable research interest in analytical community (Fan et al., 2016a; Shi et al., 2016; Shu et al., 2016) and, thus, achieved dramatic progress at a fast rate in the development of signaling strategies as well as the detection of various targets, making the PEC technique into a competitive and powerful analytical technique for methyltransferase (MTase) activity analysis (Shen et al., 2015; Wu et al., 2013; Yang et al., 2015; Yin et al., 2014). However, up to now, the reported PEC biosensors mainly depends on the compulsory and complicated chemical immobilization of bio-recognition probes onto

the surface of solid photoelectrode and/or the tedious and time-consuming covalent labeling of them onto photoactive semiconductor nanomaterials (Fan et al., 2016b; Wang et al., 2015; Xu et al., 2016). These immobilization processes significantly restricted the configurational freedom of the surface-immobilized bio-recognition probes due to the steric hindrance effect of the solid photoelectrodes or photoactive labels, resulting in low target-binding efficiency and rate (Ge et al., 2016; Hou et al., 2015; Liu et al., 2015a). To overcome the aforementioned shortcomings, rather than on the heterogeneous electrode/material interface, the whole bio-recognition as well as signal amplification processes should be carried out in the homogeneous solution without the covalent immobilization of any bio-recognition probes. This can not only maximally maintain the binding affinity and rate of the unmodified bio-recognition probes but also accelerate DNA interaction (Zhao et al., 2014a) and DNA-enzyme reaction (Xuan et al., 2012, 2013).

Herein, with the aim of developing a novel label-free homogeneous PEC biosensing platform, a water-soluble, free-base, tetracationic porphyrin (5,10,15,20-Tetrakis(N-methylpyridinium-4-yl)porphyrin, referred as TMPyP) is employed as the photoactive component in this work to photoelectrochemically detect the activity of DNA MTase. As a representative of the light-absorbing photoactive material family, porphyrin has drawn considerable research interest in photodynamic therapy (Yuan et al., 2013), photoelectronic community (Aly et al., 2014), and photoelectrochemical assay (Hu et al., 2013; Ikeda et al., 2009; Li et al., 2015; Li et al., 2016; Li et al., 2013; Shu et al., 2015; Tu et al., 2010; Tu et al., 2011; Zhao et al.,

2012) due to their outstanding optical and electrical properties of, for example, remarkably high extinction coefficients in the visible region, ultrafast electron injection, and slow charge recombination kinetics. Then, a simple photoelectrode was constructed by adsorbing TMPyP onto the surface of 1-naphthalenesulfonate anion (NS^-) grafted indium tin oxide (NS^--ITO) electrode through the convenient π–π stacking interactions as well as the electrostatic attraction. It was found that the attached free-base tetracationic TMPyP on NS^--ITO (TMPyP-NS^--ITO) shows relatively weak PEC response in the presence of ascorbic acid as the electron donor, while the pre-adsorption of single-stranded oligonucleotide (ssON) onto the surface of NS^--ITO before TMPyP attachment (TMPyP-ssON-NS^--ITO) could dramatically promote the PEC response of TMPyP under the same conditions. Furthermore, this enhancement effect exhibits high sensitivity and specificity toward ssON pre-adsorption, thus providing the basis for sensitive and label-free homogeneous PEC detection of DNA MTases activity with the aids of a compatibly designed signal transduction strategy.

In this strategy, a hairpin-shaped oligonucleotide with a long loop was constructed as the MTase substrate, the stem of which contained a specific recognition sequence for both MTase and methylation-sensitive restriction endonuclease. Here, M.SssI MTase is chosen as a proof-of-concept MTase to demonstrate the analytical performance of the proposed label-free homogeneous PEC biosensing platform. After the action of M.SssI MTase, HpaII endonuclease is employed to discriminate the unmethylated and methylated hairpin oligonucleotide substrate (HONS).

Unmethylated HONS will be cleaved by HpaII endonuclease at the middle of its duplex stem, generating three ssON fragments, which are further converted to deoxyribonucleoside 5'-monophosphates (dNMP) by exonuclease I-catalyzed ssON digestion. We found that dNMP exhibit no enhancement on the PEC response of TMPyP on account of their weak affinity toward the surface of NS^{-}-ITO electrode. In contrast, methylated HONS maintains its integrity and, thus, could be stably adsorbed onto the surface of NS^{-}-ITO electrode to enhance the PEC response of TMPyP remarkably. With the higher concentration of M.SssI MTase, the enhancement effect is more pronounced, which forms the basis for signal-on assay of M.SssI MTase, providing a wide dynamic range from 0.01 to 120 U/mL and a low detection limit of 3.5 mU/mL. Finally, we also demonstrated the applicability of the developed label-free and homogeneous PEC biosensing platform for MTase assay in complex biological matrixes as well as for reliable MTase inhibitors screening.

2. Experimental section

The Experimental section of this work are described in Supplementary information.

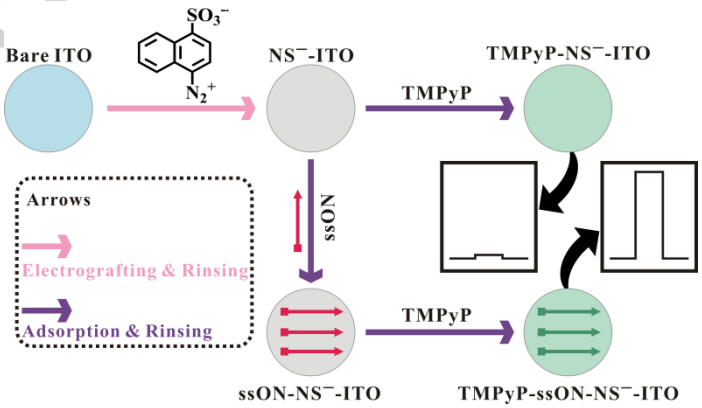

Scheme 1. Schematic illustration of the mechanism for oligonucleotide-enhanced photocurrent response of TMPyP on NS^{-}-grafted ITO electrode.

3. Results and discussion

The mechanism for oligonucleotide-enhanced photocurrent response of TMPyP on NS^--grafted ITO electrode is schematically depicted in Scheme 1. In this work, the PEC properties of the modified ITO electrodes, applied as a photoelectrode, at different modification stage were investigated by recording their time-dependent photocurrent responses upon the intermittent ~427 nm irradiation (LED light source, emission spectrum in Fig. S1) in 0.1 M PBS (pH 7.4) using 10.0 mM AA as suicidal electron donor. As shown in Scheme 1, NS^- groups are firstly electro-grafted onto the ITO electrode surface (Scheme 1). A thoroughly rinsing is always implemented to remove the loosely bounded molecules at the end of each modification/adsorption step. Fig. 1A shows that both bare ITO electrode (curve a) and NS^--ITO electrode (curve b) exhibit no photocurrent response under ~427 nm irradiation. After 15 min incubation of NS^--ITO electrode with 4.0 μM TMPyPs in 0.1 M PBS (pH 7.4), TMPyPs can be adsorbed onto the surface of NS^--ITO electrode through the convenient electrostatic interactions between the negatively charged NS^- groups on electrode interface and N-methylated pyridine groups ($^+N-CH_3$) on TMPyPs with an opposite charge as well as the π–π stacking interactions between the rings of NS^- groups and the macrocycle of TMPyPs. As expected, with the irradiation light switching on and off, an excellent cathodic photocurrent response (0.112 μA at 0 V vs. Ag/AgCl) was observed (curve c) from the as-fabricated TMPyP-NS^--ITO electrode. Moreover, as presented in Fig. 1A, the photocurrent from TMPyP-NS^--ITO electrode responded promptly following the onset and offset of the irradiation light, suggesting

the fast photo-induced electron charge excitation, separation and transfer on the electrode interface. Furthermore, the photocurrent response of the obtained TMPyP-NS^{-}-ITO electrode could be repeatedly regenerated every 10 seconds without any noticeable decay within 50 on/off illumination cycles (Fig. S2), suggesting good operational stability for sensitive and reliable signal collection.

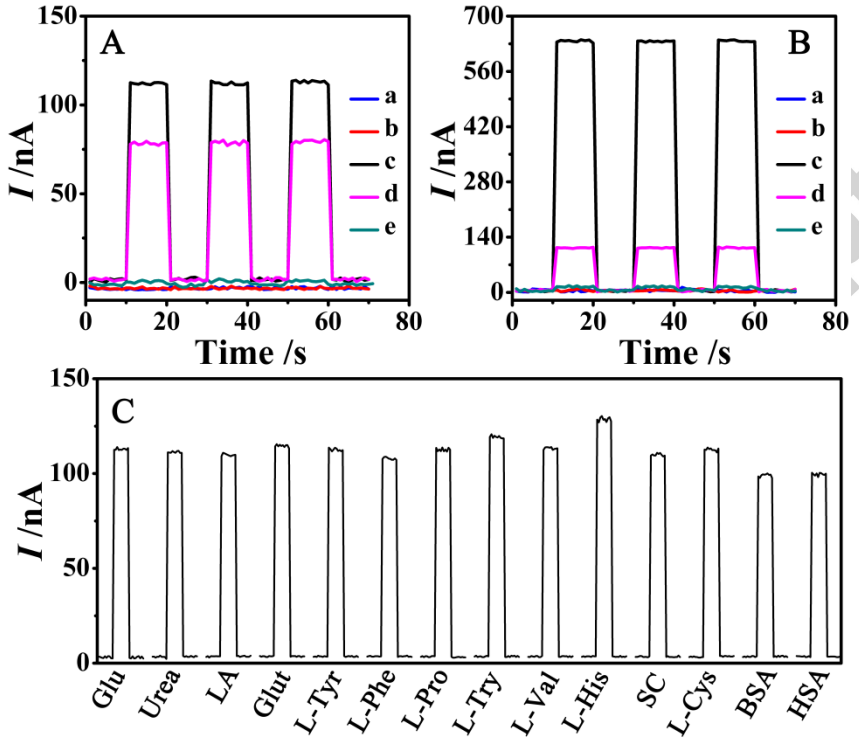

Fig. 1. (A) Photocurrent response of (a) bare ITO, (b) NS^{-}-ITO, (c, e) TMPyP-NS^{-}-ITO, and (d) RON-TMPyP-NS^{-}-ITO. (B) Photocurrent response of (a) RON-NS^{-}-ITO, (b) buffer-NS^{-}-ITO. (c, e) TMPyP-RON-NS^{-}-ITO, and (d) TMPyP-buffer-NS^{-}-ITO. (C) Photocurrent response of TMPyP-X-NS^{-}-ITO electrodes, X (from left to right) = 1.0 mM glucose (Glu), 1.0 mM urea, 1.0 mM lactic acid (LA), 1.0 mM glutathione (Glut), 1.0 mM L-tyrosine (L-Tyr), 1.0 mM L-phenylalanine (L-Phe), 1.0 mM L-proline (L-Pro), 1.0 mM L-tryptophan (L-Try), 1.0 mM L-valine (L-Val), 1.0 mM L-histidine (L-His), 1.0 mM sodium citrate (SC), 1.0 mM L-cysteine (L-Cys), 1.0 mg/mL bovine serum albumin (BSA), or 1.0 mg/mL human serum albumin (HSA). The PEC tests were performed at 0.0 V (vs. Ag/AgCl) applied voltage under ~470 nm excitation light in 0.1 M PBS (pH 7.4) with (a-d) or without (e) 0.01 M AA. The concentration of TMPyP and RON was 4.0 μM and 1.5 μM, respectively.

In this work, we found that the pre-adsorption of random ssON (RON, Table S1) onto the surface of NS^{-}-ITO (denoted as RON-NS^{-}-ITO) before TMPyP adsorption could remarkably enhance the PEC response of TMPyP. The stable adsorption of

ssON onto the surface of NS^--ITO electrode has been demonstrated in our previous work (Ge et al., 2017), which is attributed to the strong π–π stacking interactions between the ring structures in the nucleobases and the bihexagonal cells of naphthalene in NS^- groups. Upon incubation of NS^--ITO electrode in 10 mM Tris-HCl buffer (pH 7.4) with or without 1.5 μM RON for 30 min at 37 °C, respectively, as shown in Fig. 1B, both the as-fabricated RON-NS^--ITO electrode (curve a) and buffer-NS^--ITO electrode (curve b) generated no photocurrent output. After the adsorption of TMPyPs, a significant increase in photocurrent intensity (0.638 μA at 0 V vs. Ag/AgCl) was only observed on the resulted TMPyP-RON-NS^--ITO electrode (Fig. 1B, curve c) with fast and stable photo-response (Fig. S2), which represented about 5-times higher than that on TMPyP-buffer-NS^--ITO electrode (Fig. 1B, curve d). This fact suggested that the pre-adsorption of ssON could enhance the photocurrent signal of the TMPyPs on NS^--ITO electrode effectively. In order to verify that the photocurrent enhancement of TMPyP is arisen from the pre-adsorption of ssON, a series of comparative trials have been implemented under the same experimental conditions. The purple line in Fig. 1A is the photocurrent response of the TMPyP-NS^--ITO electrode after the post-adsorption of ssON. Compared with that of TMPyP-NS^--ITO (Fig. 1A, curve c), an obvious decrease in photocurrent intensity was observed on RON-TMPyP-NS^--ITO electrode (Fig. 1A, curve d), indicating that the post-adsorption of ssON shows no enhancement on the photocurrent response of TMPyP on NS^--ITO electrode. Additionally, we further monitored whether the

pre-adsorption of other biological species on NS^--ITO electrode could cause the photocurrent enhancement of TMPyP. As seen from Fig. 1C, the photocurrent responses of TMPyP-X-NS^--ITO electrodes (X = glucose, urea, lactic acid, glutathione, L-tyrosine, L-phenylalanine, L-proline, L-tryptophan, L-valine, L-histidine, sodium citrate, L-cysteine, bovine serum albumin, or human serum albumin) are almost the same as that of TMPyP-NS^--ITO electrode (Fig. 1A, curve a), suggesting a high specificity of this photocurrent enhancement mechanism towards ssON, which is an important prerequisite for the development of sensitive homogeneous PEC biosensing platform. Moreover, the photocurrent enhancement of TMPyP also shows high dependence on the adsorption time as well as the sequence of the ssON (Fig. S3), which is consistent with the phenomenon observed in our previous work (Ge et al., 2017), indicating that the PEC response of TMPyP on NS^--ITO electrode is sensitive to the amount of pre-adsorbed ssON.

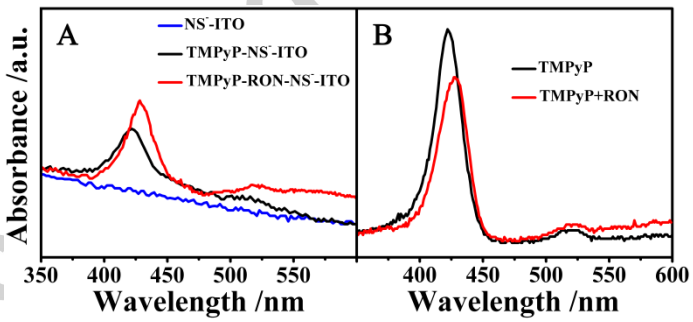

Fig. 2. (A) Absorption spectra of NS^--ITO (blue), TMPyP-NS^--ITO (black), and TMPyP-RON-NS^--ITO (red). The concentration of TMPyP and RON was 4.0 μM and 1.5 μM, respectively. (B) Absorption spectra of 4.0 μM TMPyP in 0.1 M PBS (pH 7.4) with (red) or without (black) 1.5 μM RON.

To get an in-depth understanding of the principle of this photocurrent enhancement phenomenon, we investigated the photocurrent response of modified NS^--ITO electrodes in PBS aqueous solution without the addition of AA. In this case,

the photocurrent response of both TMPyP-NS^--ITO electrode (Fig. 1A, curve e) and TMPyP-RON-NS^--ITO electrode (Fig. 1B, curve e) could be negligible, excluding the possibility of pre-adsorbed ssON acting as electron donor to effectively enhance the photocurrent of TMPyP. Another possibility is the molecular interplay between TMPyP and ssON, which has been similarly reported in the case of copper(II)-containing form of TMPyP and short oligonucleotide in homogeneous solution (Gaier et al., 2014). In order to examine the interaction between TMPyP molecules and RON on NS^--ITO electrode, we first recorded the absorption spectra of NS^--ITO electrode before and after the incubation in 4.0 μM TMPyP aqueous solution. As shown in Fig. 2A, NS^--ITO electrode did not exhibit any obvious absorption peak between 350 and 600 nm, whereas the TMPyP-NS^--ITO electrode exhibit an intense absorption band at ~422 nm, which is well consistent with the characteristic Soret band of 4.0 μM TMPyP solution (Fig. 2B), further confirming the successful attachment of TMPyP on NS^--ITO. Upon subjecting the NS^--ITO electrode to the solution of 1.5 μM RON before TMPyP adsorption, the Soret band of the resulted TMPyP-RON-NS^--ITO electrode exhibits a bathochromic shift up to 6 nm compared to that of TMPyP-NS^--ITO electrode (Fig. 2A). As is evident in Fig. 2B, the observed red-shift of TMPyP Soret band were in good agreement with the absorption characteristics of TMPyP molecules in 1.5 μM RON solution and, thus, suggested a strong interaction between TMPyP and RON adsorbed on NS^--ITO electrode. Moreover, Fig. 2A reveals that, on RON-NS^--ITO electrode surface, TMPyP shows an obvious hyperchromicity (~57%), rather than a hypochromicity (~23%) in the

solution of RON (Fig. 2B). The reason might be most likely a consequence of the fact that, in the presence of pre-adsorbed RON, more TMPyP molecules could be attached onto the electrode surface due to the aforementioned strong binding interactions with RON. Therefore, the observed remarkable photocurrent enhancement should be ascribed to the following possible reasons: (i) As shown in Fig. S1, the spectrum of the LED light source exhibits a maximum emission wavelength at about 427 nm, at which the TMPyP-ssON-NS^{-}-ITO electrode with a Soret band of ~428 nm could be excited more effectively in comparison to TMPyP-NS^{-}-ITO electrode, leading to a higher photocurrent conversion efficiency. (ii) Compared with NS^{-}-ITO electrode, more TMPyP molecules could be attached onto the surface of NS^{-}-ITO electrode with the aids of pre-adsorbed ssON to produce photo-induced electron-hole separation.

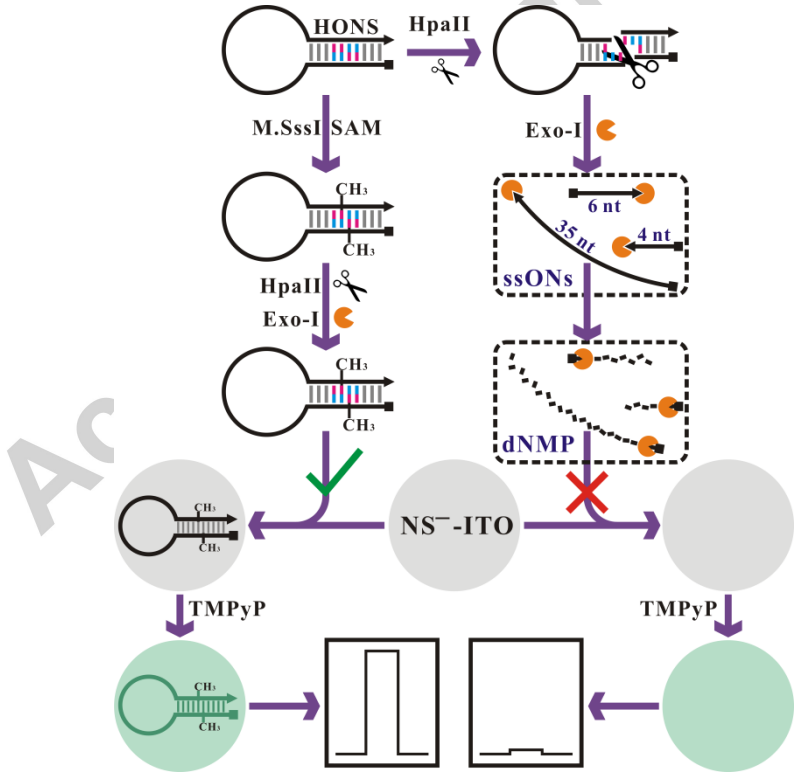

Scheme 2. Schematic illustration of the principle for the label-free homogeneous PEC biosensing platform for M.SssI MTase activity analysis.

Since the extent of photocurrent increase associates intimately and specifically

with the concentration of pre-adsorbed ssON, a novel label-free homogeneous PEC biosensing platform for M.SssI MTase activity analysis can be tailored by recording the methylation-controlled photocurrent variation. The overall sensing principle of this label-free homogeneous PEC biosensor, with the employment of HONS as recognition probe and TMPyP as the photoactive component, is illustrated schematically in Scheme 2. The designed HONS can self-hybridize into a stable stem-loop structure with a short duplex stem (10 base-pair, bp) and a long ssON loop (25 nucleotide, nt, Table S1), with the aids of which HONS can be firmly adsorbed onto NS^{-}-ITO electrode surface to induce the photocurrent enhancement of TMPyP (Fig. 3, curve a). At the middle of the duplex stem in HONS, there is a palindromic sequence of 5'-C-C-G-G-3' (colored in blue and red), which could be specifically recognized by both M.SssI MTase and HpaII endonuclease. As shown in Scheme 2, in the absence of M.SssI MTase, no HONS is methylated. Then, HpaII endonuclease could specifically recognize the unmethylated palindromic sequence in the stem of HONS and cleave it into two portions at the recognition site between the cytosines (5'-C-|-C-G-G-3'). One portion is a neo-hairpin structural oligonucleotide with a 25 nt loop and a 4-bp duplex terminal. The other one is a 4-bp duplex. According to the melting temperature (T_m) value calculation equation (T_m = 4 °C × G/C pair + 2 °C × A/T pair), the newly generated short duplex only had a T_m of 14 °C and will be dehybridized into two short ssON fragments (4 nt and 6 nt, respectively, Table S1) at the reaction temperature (37 °C), both of which are hardly adsorbed onto the NS^{-}-ITO electrode surface (Ge et al., 2017), leading to low photocurrent responses (Fig. S4A,B,

curve a). Similarly, the generated new hairpin oligonucleotide containing a 4 bp stem is also unstable at the reaction temperature (37 °C) and can be changed into a 35 nt ssON (Table S1), which, however, could be easily adsorbed onto the surface of NS^{-}-ITO electrode, inducing a remarkable enhancement of the PEC response of TMPyP (Fig. S4C, curve a). In order to minimize this background signal (Fig. 3, curve b) as much as possible, exonuclease I (Exo-I)-catalyzed digestion is incorporated into this strategy to completely digest the cleaved HONS into dNMP (Scheme 2), which show weak affinity toward the surface of NS^{-}-ITO electrode and, thus, exhibit low enhancement on the PEC response of TMPyP (Fig. S4, curve b and Fig. 3, curve c). In the presence of M.SssI MTase, as seen in Scheme 2, it can recognize the sequence of 5'-C-C-G-G-3' in the duplex stem of HONS and facilitate the exchange of a methyl group from SAM to the underlined cytosine, forming 5'-C-C^{m}-G-G-3', which is known to block the cleavage reaction by the HpaII endonuclease (Li et al., 2012; Liu et al., 2015b; Wang et al., 2012). In addition, the blunt end of the duplex stem endows the HONS with high resistance against digestion by Exo-I. Thus, methylated HONS maintains its ability of photocurrent enhancement towards TMPyP on NS^{-}-ITO electrode surface (Fig. 3, curve d). Obviously, according to the procedure, the amount of methylated HONS is in principle proportional to the activity of M.SssI MTase. With growing the amount of M.SssI MTase, more HONS could be firmly adsorbed onto the surface of NS^{-}-ITO electrode, which resulted in an elevated photocurrent to reflect the methylation event and M.SssI MTase activity. As expected, with the increase of M.SssI MTase concentration, enhanced photocurrent

intensity was observed (Fig. 3, curve e and f), confirming the feasibility of the proposed homogeneous PEC biosensing platform for M.SssI MTase activity analysis.

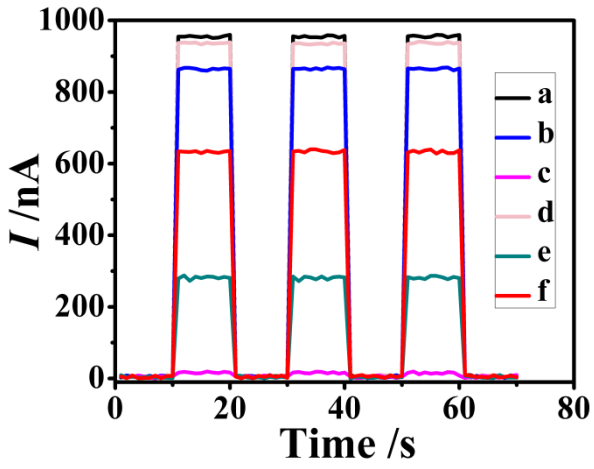

Fig. 3. (a) Photocurrent response of TMPyP-X-NS^{-}-ITO electrodes, X = HONS (a); HONS + HpaII (b); HONS + HpaII + Exo-I (c); methylated HONS + HpaII + Exo-I (d); 0.08 U/mL M.SssI + HONS + HpaII + Exo-I (e); 3.0 U/mL M.SssI + HONS + HpaII + Exo-I (f). The concentration of HONS, HpaII, Exo-I, and TMPyP was 2.0 μM, 10 U/mL, 5.0 U/mL, and 4.0 μM, respectively.

The aforementioned methylation-controlled photocurrent response of the proposed homogeneous PEC biosensing platform prompted us to evaluate its analytical capability for signal-on M.SssI MTase activity analysis. In this case, HONSs were methylated with different concentrations of M.SssI MTase, followed by treatment with HpaII endonuclease and Exo-I according to the experimental protocol described in the Experimental Section. Fig. 4A records the corresponding variance of photocurrent intensities of TMPyP on NS^{-}-ITO electrode in response to above reaction mixtures under the same conditions. We observed that the photocurrent intensity increased gradually with the increasing of M.SssI MTase concentration. This increase was in accordance with the fact that the presence of more M.SssI MTase caused the methylation of more HONSs, after which the methylated HONSs, with high resistant to HpaII cleavage and Exo-I digestion, are firmly adsorbed on the

surface of NS^{-}-ITO electrode, enhancing the photocurrent of post-adsorbed TMPyPs. A plot of the photocurrent intensities versus the logarithm (lg) of M.SssI MTase concentrations are derived in Fig. 4B, which revealed a linear correlation in the dynamic range from 0.01 to 120 U/mL. The corresponding linear regression equation was expressed as $\Delta I = 187.78\lg c_{M.SssI} + 514.87$ (unit of $c_{M.SssI}$ is U/mL) with a correlation coefficient of 0.9959. The detection limit was estimated to be 3.5 mU/mL (3σ), which was comparable to or lower than that of many other reported M.SssI MTase activity analysis (Table S2). In addition, each data point in the calibration curve represents six repetitive and parallel measurements of M.SssI MTase using independent NS^{-}-ITO electrodes, which show the relative standard deviations (n = 6) ranging from 2.73% to 9.81%, indicating an acceptable reproducibility of the proposed homogeneous PEC biosensing platform. Moreover, to investigate the specificity of the proposed method, HaeIII, AluI, and HhaI were employed as the potential interference MTase, which can methylate the underlined cytosine within the double-stranded symmetric tetranucleotide sequence of 5'-G-G-C-C-3', 5'-A-G-C-T-3', and 5'-G-C-G-C-3', respectively. As summarized in Fig. 4C, the increment of photocurrent intensity caused by 50 U/mL HaeIII, 50 U/mL AluI, or 50 U/mL HhaI is very similar to that of the MTase-free test. In contrast, only 1.0 U/mL M.SssI MTase can cause an significant change in the photocurrent intensity under the same experimental conditions, suggesting that the proposed homogeneous PEC biosensing platform has an excellent selectivity for M.SssI MTase activity assays. From above facts, it is credible that the developed homogeneous PEC biosensing

platform can effectively conduct the selectively quantitative activity assay of the M.SssI MTase with desirable sensitivity and reproducibility.

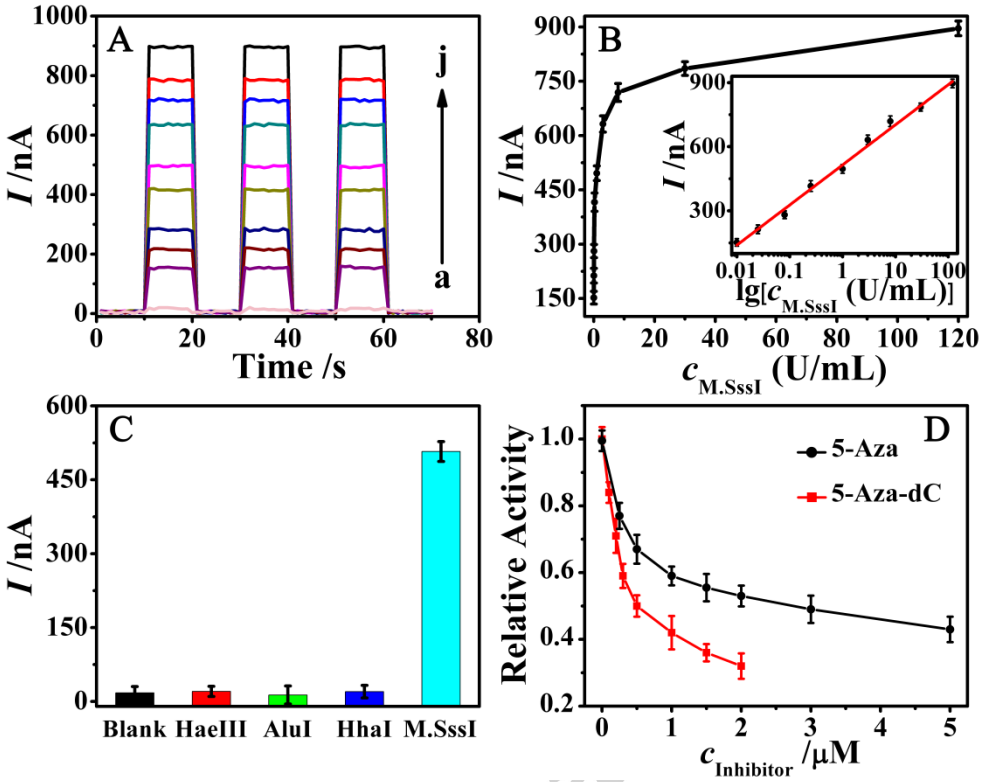

Fig. 4. (A) Photocurrent responses of the proposed label-free homogeneous PEC biosensing platform to different concentrations of M.SssI MTase (from a to j: 0, 0.01, 0.025, 0.08, 0.25, 1.0, 3.0, 8.0, 30, and 120 U/mL). (B) The linear relationship of the photocurrent intensity (*I*) versus the logarithmic value of M.SssI MTase concentration. (C) Selectivity investigation of the proposed label-free homogeneous PEC biosensing platform using HaeIII, AluI, and HhaI as interference MTase. The concentration of M.SssI MTase is 1.0 U/mL. The concentration of each interference MTase is 50 U/mL. (D) The inhibition effect of 5-Aza and 5-Aza-dC on M.SssI MTase activity.

After confirming the analytical performance of the proposed homogeneous PEC biosensing platform for M.SssI MTases activity analysis, the inhibitor screening capacity of which was evaluated through challenging the M.SssI MTases solution to two typical inhibitors, i.e. 5-Aza and 5-Aza-dC, respectively, at desired concentrations. Then, the M.SssI MTase activity was determined as described in the Experimental section. The experimental results (not shown here) indicate that the two drugs exhibited negligible influence on the activity of both HpaII and Exo-I when the dose

of 5-Aza and 5-Aza-dC is lower than 5.0 and 2.0 uM, respectively. Thus, 5-Aza and 5-Aza-dC at the concentration of lower than 5.0 and 2.0 μM, respectively, were used in this study to investigate their influence on the relative activity of M.SssI MTase, which was quantitatively calculated by the following equation:

$$\text{Relative Activity} = [I_2 - I_0]/[I_1 - I_0]$$

where I_0 and I_1 are the photocurrent intensities in the absence or presence of 120 U/mL M.SssI MTase, respectively, and I_2 refers to the photocurrent intensities in the presence of both 120 U/mL M.SssI MTase and inhibitors at various dose. Fig. 4D shows that the relative activity of M.SssI MTases decreased remarkably with the increasing concentration of the inhibitors in an obvious dose-dependent manner, based on which the IC_{50} values (the inhibitor concentration required to reduce M.SssI activity by 50%) were calculated to be 0.5 μM and 2.8 μM for 5-Aza-dC and 5-Aza, respectively. Obviously, 5-Aza-dC exhibited higher inhibitory effect than that of 5-Aza, which were consistent with the previous reports (Li et al., 2012; Zhao et al., 2016). Therefore, we might conclude that our proposed homogeneous PEC biosensing platform can be considered as a potential scheme for practical application in MTase inhibitors screening that may serve to anticancer drug discovery.

4. Conclusions

In summary, this work explored the oligonucleotide-modulated photocurrent enhancement mechanism of TMPyP on NS^{-}-ITO electrode and demonstrated its application as a versatile homogeneous PEC biosensing platform for, as a proof-of-concept, label-free M.SssI MTase activity analysis. Control experiments

were carried out and reached the conclusion that this robust photocurrent enhancement phenomenon might be attributed to the strong molecular interaction between TMPyP and oligonucleotide, which not only improve the matching degree between the Soret band of TMPyP and the maximum emission wavelength of LED light source but also benefit to increase the loading amounts of TMPyP molecules on NS^{-}-ITO electrode. For the achievement of sensitive assay of M.SssI MTase activity, a compatible signal transduction strategy is rationally developed through the combined use of enzymatic cleavage of the HONSs by HpaII endonuclease and the subsequent digestion of the reaction product by Exo-I to minimize the background signal as much as possible. The proposed PEC biosensing platform features not only the first use of TMPyP as high efficient photoactive component but also the implementation of both target recognition and enzymatic reaction in homogeneous solution. More importantly, the mechanism revealed here is expected not only to offer new opportunities for the development of label-free homogeneous PEC biosensing platform, but also to inspire more interests in the design and construction of novel signaling routs for advanced homogeneous PEC bioanalysis with faster response, enhanced sensitivity, and higher stability.

ACKNOWLEDGEMENTS

This work was financially supported by National Natural Science Foundation of China (31501570, and 21575074, and 21775083), Research Foundation for Distinguished Scholars of Qingdao Agricultural University (663-1115003), The Major Basic Research Program of Natural Science Foundation of Shandong Province (No.

ZR2018ZC0127), and The Special Foundation for Distinguished Taishan Scholar of Shandong Province (ts201511052).

REFERENCES

Aly, S.M., Parida, M.R., Alarousu, E., Mohammed, O.F., 2014. Chem. Commun. 50, 10452-10455.

Fan, G.-C., Shi, X.-M., Zhang, J.-R., Zhu, J.-J., 2016a. Anal. Chem. 88, 10352-10356.

Fan, G.-C., Zhu, H., Du, D., Zhang, J.-R., Zhu, J.-J., Lin, Y., 2016b. Anal. Chem. 88, 3392-3399.

Gaier, A.J., Ghimire, S., Fix, S.E., McMillin, D.R., 2014. Inorganic Chemistry 53, 5467-5473.

Ge, L., Wang, W., Sun, X., Hou, T., Li, F., 2016. Anal. Chem. 88, 2212-2219.

Ge, L., Wang, W., Li, F., 2017. Anal. Chem. 89, 11560-11567.

Hou, T., Li, W., Liu, X., Li, F., 2015. Anal. Chem. 87, 11368-11374.

Hu, Y., Xue, Z., He, H., Ai, R., Liu, X., Lu, X., 2013. Biosens. Bioelectron. 47, 45-49.

Ikeda, A., Nakasu, M., Ogasawara, S., Nakanishi, H., Nakamura, M., Kikuchi, J.-i., 2009. Organic Letters 11, 1163-1166.

Jiang, D., Du, X., Zhou, L., Li, H., Wang, K., 2017. Anal. Chem. 89, 4525-4531.

Li, H., Mu, Y., Yan, J., Cui, D., Ou, W., Wan, Y., Liu, S., 2015. Anal. Chem. 87, 2007-2015.

Li, M., Zheng, Y., Liang, W., Yuan, Y., Chai, Y., Yuan, R., 2016. Chem. Commun. 52, 8138-8141.

Li, W., Wu, P., Zhang, H., Cai, C., 2012. Anal. Chem. 84, 7583-7590.

Li, X., Zhu, L., Zhou, Y., Yin, H., Ai, S., 2017. Anal. Chem. 89, 2369-2376.

Li, Y.-J., Ma, M.-J., Yin, G., Kong, Y., Zhu, J.-J., 2013. Chem. Eur. J. 19, 4496–4505.

Liu, X., Li, W., Hou, T., Dong, S., Yu, G., Li, F., 2015a. Anal. Chem. 87, 4030-4036.

Liu, Y., Wei, M., Zhang, L., Wei, W., Zhang, Y., Liu, S., 2015b. Chem. Commun. 51, 14350-14353.

Mei, L.-P., Liu, F., Pan, J.-B., Zhao, W.-W., Xu, J.-J., Chen, H.-Y., 2017. Anal. Chem. 89, 6300-6304.

Shen, Q., Han, L., Fan, G., Abdel-Halim, E.S., Jiang, L., Zhu, J.-J., 2015. Biosens. Bioelectron. 64, 449-455.

Shi, X.-M., Fan, G.-C., Shen, Q., Zhu, J.-J., 2016. ACS Appl. Mater. Interfaces 8, 35091-35098.

Shu, J., Qiu, Z., Zhuang, J., Xu, M., Tang, D., 2015. ACS Appl. Mater. Interfaces 7, 23812-23818.

Shu, J., Qiu, Z., Zhou, Q., Lin, Y., Lu, M., Tang, D., 2016. Anal. Chem. 88, 2958-2966.

Tu, W., Dong, Y., Lei, J., Ju, H., 2010. Anal. Chem. 82, 8711-8716.

Tu, W., Lei, J., Wang, P., Ju, H., 2011. Chem. Eur. J. 17, 9440-9447.

Tu, W., Cao, H., Zhang, L., Bao, J., Liu, X., Dai, Z., 2016. Anal. Chem. 88, 10459-10465.

Wang, J., Liu, Z., Hu, C., Hu, S., 2015. Anal. Chem. 87, 9368-9375.

Wang, M., Xu, Z., Chen, L., Yin, H., Ai, S., 2012. Anal. Chem. 84, 9072-9078.

Wu, Y., Zhang, B., Guo, L.-H., 2013. Anal. Chem. 85, 6908-6914.

Xu, F., Zhu, Y.-C., Ma, Z.-Y., Zhao, W.-W., Xu, J.-J., Chen, H.-Y., 2016. Chem. Commun. 52, 3034-3037.

Xuan, F., Luo, X., Hsing, I.M., 2012. Anal. Chem. 84, 5216-5220.

Xuan, F., Luo, X., Hsing, I.M., 2013. Anal. Chem. 85, 4586-4593.

Yang, Z., Wang, F., Wang, M., Yin, H., Ai, S., 2015. Biosens. Bioelectron. 66, 109-114.

Yin, H., Sun, B., Zhou, Y., Wang, M., Xu, Z., Fu, Z., Ai, S., 2014. Biosens. Bioelectron. 51, 103-108.

Yuan, Q., Wu, Y., Wang, J., Lu, D., Zhao, Z., Liu, T., Zhang, X., Tan, W., 2013. Angew. Chem. Int. Ed. 52, 13965-13969.

Zang, Y., Lei, J., Ju, H., 2017. Biosens. Bioelectron. 96, 8-16.

Zhao, H., Wang, L., Jiang, W., 2016. Chem. Commun. 52, 2517-2520.

Zhao, J., Hu, S., Zhong, W., Wu, J., Shen, Z., Chen, Z., Li, G., 2014a. ACS Appl. Mater. Interfaces 6, 7070-7075.

Zhao, W.-W., Zhang, L., Xu, J.-J., Chen, H.-Y., 2012. Chem. Commun. 48, 9456-9458.

Zhao, W.-W., Xu, J.-J., Chen, H.-Y., 2014b. Chem. Rev. 114, 7421-7441.

Zheng, Y.-N., Liang, W.-B., Xiong, C.-Y., Yuan, Y.-L., Chai, Y.-Q., Yuan, R., 2016. Anal. Chem. 88, 8698-8705.

Highlights

1. The first use of TMPyP as photoactive component in photoelectrochemical biosensing.

2. Oligonucleotide-modulated photocurrent enhancement of TMPyP is investigated on 1-naphthalenesulfonate anion grafted ITO electrode.

3. A label-free homogeneous photoelectrochemical biosensing platform is demonstrated.

4. Sensitive methyltransferase activity assay and reliable methyltransferase inhibitors screening is realized.